Rare Met.
https://doi.org/10.1007/s12598-022-02218-4

RARE METALS

ORIGINAL ARTICLE

Promoted Li^+ conduction in PEO-based all-solid-state electrolyte by hydroxyl-modified glass fiber fillers

Xin Wang, Xiu Shen, Peng Zhang, Ai-Jun Zhou*, Jin-Bao Zhao*

Received: 31 January 2022 / Revised: 25 April 2022 / Accepted: 29 April 2022

Abstract In the polyoxyethylene (PEO)-based solid-state electrolytes, the low ionic conductivity of lithium ions limits its application in solid-state lithium batteries, so optimizing the conduction path of lithium ions is beneficial to improve the ionic conductivity. In this work, we report the use of hydrothermal carbon nano-sphere (HCS) modified glass fibers (GF) as a functional filler (GF@HCS) to improve the ionic conductivity of PEO composite solid-state electrolytes. The oxygen atoms in the hydroxyl groups on the surface of HCS can be complexed with Li ions as its transport sites, which means that it can promote the long-distance transport of Li ions along the glass fiber surface. With addition of 2 wt% GF@HCS fillers, the degree of crystallinity of PEO composite solid-state electrolyte is the smallest, and the ionic conductivity is significantly increased from 8.9×10^{-5} to 4.4×10^{-4} S·cm^{-1} at 60 °C. Moreover, the PEO composite solid-state electrolyte exhibits better lithium–metal interface stability in symmetric lithium batteries and superior rate performance in $LiFePO_4$ solid-state batteries.

Keywords Filler modification; Hydrothermal carbon spheres; Transport channel; Polyoxyethylene (PEO) composite electrolyte; All-solid-state battery

1 Introduction

Lithium-ion batteries (LIBs) are widely used as energy storage devices due to their high energy density. Meanwhile, as its energy density continues to increase, its safety is facing challenges due to the use of flammable liquid ester electrolytes [1, 2]. Among many strategies for improving the safety of LIBs, the use of solid-state electrolytes is intensively attempted due to their non-flammability [3–5]. In particular, polymer-based solid-state electrolytes have attracted significant attention due to their low cost, good processing performance and interface contact, among which polyoxyethylene (PEO) polymer electrolyte is the most widely studied candidate [5–9]. The oxygen atoms in the ether oxygen segment of PEO can be complexed with Li^+, so Li^+ will undergo complexation–decomplexation–complexation processes between different oxygen atoms along with the movement of the polymer segment, thereby realizing the migration of Li^+ in the PEO matrix [10–13].

Because PEO is a semi-crystalline polymer, and it is generally believed that the conduction of Li^+ mainly occurs in the amorphous region of PEO [6, 14, 15],

X. Wang, A.-J. Zhou*
Yangtze Delta Region Institute (Huzhou), University of Electronic Science and Technology of China, Huzhou 313001, China
e-mail: zhouaj@uestc.edu.cn

X. Shen, J.-B. Zhao*
State Key Laboratory of Physical Chemistry of Solid Surfaces, Collaborative Innovation Centre of Chemistry for Energy Materials, State-Province Joint Engineering Laboratory of Power Source Technology for New Energy Vehicle, Engineering Research Center of Electrochemical Technology, Ministry of Education, College of Chemistry and Chemical Engineering, Xiamen University, Xiamen 361005, China
e-mail: jbzhao@xmu.edu.cn

P. Zhang
College of Energy and School of Energy Research, Xiamen University, Xiamen 361102, China

A.-J. Zhou
School of Materials and Energy, University of Electronic Science and Technology of China, Chengdu 611731, China

Published online: 12 December 2022

nanoparticle fillers (Al_2O_3, SiO_2, TiO_2, etc.) are usually added to inhibit the formation of crystalline phases in PEO as a method to increase the ionic conductivity [16–19]. However, the promotion in ionic conductivity by these nanoparticle fillers has a certain limitation. For example, adding too much fillers will form a solvent effect which will adversely reduce the ionic conductivity of the composite electrolyte [18, 20]. Researchers also studied the effect of different morphologies of fillers on PEO solid-state electrolytes. It's found that, compared with nanoparticle fillers, one-dimensional nanowire fillers can better reduce the crystallinity of PEO, and the nanowires are more likely to form long-range ion transport channels at their interfaces, which is more favorable for the ion migration [21–23]. For example, Sheng et al. [24] reported that the addition of magnesium borate nanowires can enhance the ionic conductivity as well as the electrochemical window and mechanical properties of PEO solid-state electrolytes. The interaction between magnesium borate and anion bis(trifluoromethane)sulforimide ($TFSI^-$) increased the ionic conductivity to 3.7×10^{-4} S·cm^{-1} at 50 °C. Miller et al. used halloysite nanotube (HNT) as fillers to prepare the composite electrolyte [25]. The positively charged HNT on the surface can promote the dissociation of lithium salt, and the ionic conductivity reached 1.11×10^{-4} S·cm^{-1} at 25 °C after addition of 10% HNT. Lu et al. prepared a salt-rich composite electrolyte by introducing $Li_{6.75}La_3Zr_{1.75}Ta_{0.25}O_{12}$ (LLZTO) nanofibers into a salt-rich PEO6-LiTFSI solid-state electrolyte, which showed an ionic conductivity of 2.13×10^{-5} S·cm^{-1} at 25 °C [22]. These work all indicate that the interface of nanowires is essentially important for the long-range ion conduction in PEO matrix.

In our previous work [26], we reported that the oxygen atoms in the hydroxyl group could be complexed with Li^+ through the phenolic resin nano-spheres fillers, and interact with the PEO segment to achieve Li^+ transport. In order to further improve the conductivity of PEO-based solid-state electrolyte, modification of the hydroxyl or/and other oxygen-containing groups on the surface of the fillers is still necessary. In this work, we use glass fiber (GF) as the nanowire filler, which is further modified by hydrothermal carbon spheres (HCS) on its surface. Glass fiber is an inexpensive and easily available long-range fibrous material, while the hydrothermal carbon spheres are rich in oxygen-containing groups on the surface [27], such as hydroxyl, ester and other oxygen-containing hydrophilic groups. The hydroxyl-rich HCS were grown on the surface of glass fibers and then were added into the PEO system as a functional filler (GF@HCS). The electrochemical properties of the composite electrolyte were studied in detail. It is believed that the hydroxyl groups on the surface of the modified GF@HCS fillers can build plenty of long-range Li^+ transport channels, which greatly promoted the Li^+ conduction in the PEO-based electrolyte.

2 Experimental

2.1 Preparation of GF@HCS

The preparation process of GF@HCS composite electrolyte is illustrated in Fig. 1. Typically, 0.42 g glass fiber filter membrane (Whatman) was added to 200 ml deionized water for ultrasonic dispersion, and then 1 ml 20 wt% poly(diallyldimethylammonium chloride) solution (PDDA, Aladdin) was added, stirred for 2 h, and then filtered to obtain the dispersed glass fibers. For the growth of HCS, the dispersed glass fibers were added to a polytetrafluoroetylene (PTFE) hydrothermal reactor followed by addition of 1 g glucose and 50 ml deionized water. The hydrothermal reactor was sealed and placed in an oven at 180 °C for 24 h. After cooling, it was washed thoroughly with deionized water and ethanol and then filtered. The obtained brown GF@HCS product was finally dried in vacuum at 100 °C for 24 h before use. Additional, pure HCS was synthesized under the same conditions without the addition of GF.

2.2 Composite solid-state electrolyte

PEO (60w, BASF) and $LiClO_4$ (Aladdin) with the molar ratio of 16 (denoted as PEO16) were dissolved in anhydrous acetonitrile (Aladdin) to form a solution (10 wt%). Then different amounts of unmodified GF or GF@HCS (2 wt%, 4 wt%, 6 wt%) were added into the above solution. After sufficient stirring, the solution was placed in the PTFE mold to volatilize the acetonitrile solvent. The as-formed film was then dried in vacuum at 50 °C for 24 h to remove the residual solvent, resulting in the final composite solid-state electrolyte membrane.

2.3 Assembly and test of solid-state batteries

Firstly, the composite binder was prepared. PEO and $LiClO_4$ with the molar ratio of 16 were added into the N,N-dimethylformamide (DMF, Aladdin) solvent, then PVDF powder was added, and the weight ratio of PEO–PVDF was kept at 7:3. Then the mixture was stirred and dissolved to form a solution with a weight ratio of 10%. Then, according to the weight ratio of 6:2:2, $LiFePO_4$, composite binder and acetylene black were added into DMF solvent, mixed and stirred, and then the slurry was coated on aluminum foil, vacuum dried at 60 °C for 24 h. The loading density of $LiFePO_4$ was controlled at about 1.0 mg·cm^{-2}. The $LiFePO_4$ solid-state cells were assembled in 2032-type

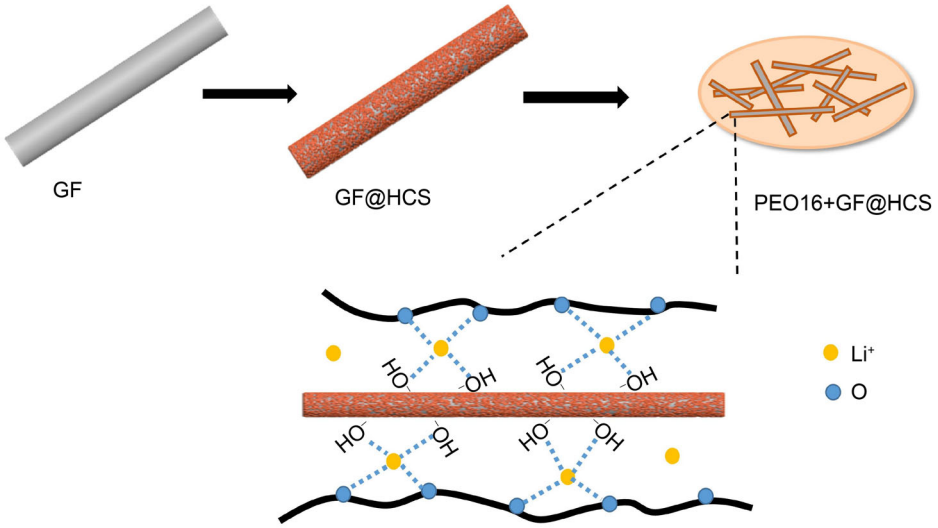

Fig. 1 Schematic diagram of composite electrolyte preparation and mechanism of Li^+ conduction

coin cell with lithium metal sheet as the negative electrode and using the as-prepared composite electrolyte membrane as the middle layer. The voltage range of for the charge/discharge test was 2.5–3.8 V, whereas the charging and discharging current was set as 0.5C, respectively (1.0C = 150 mAh·g^{-1}). Rate characteristics of the cells were tested beginning with 0.5C cycling and then followed by cycling at 0.5C, 1.0C, 2.0C, 4.0C and finally returned to 0.5C, respectively.

2.4 Material characterization and electrochemical tests

The morphology of samples was observed by field electron-scanning electron microscopy (SEM, Zeiss GeminiSEM 500). The molecular structure information was detected by Fourier transform infrared spectroscopy (FTIR, Nicolet IS5). The thermal behaviors of composite electrolyte were evaluated by synchronous thermal analyzer (STA 449 F3, Netzsch). The melting temperatures (T_m) and apparent melting enthalpy (ΔH_m) were determined from the endothermic peaks, and the degree of crystallinity (X) of composite electrolyte was calculated from the following equation:

$$X = \Delta H_{m,PEO}/(f_{PEO} \times \Delta H_{PEO}) \quad (1)$$

where f_{PEO} is the weight ratio of PEO in the related composite electrolyte, $\Delta H_{m,PEO}$ is the apparent melting enthalpy of the composite electrolyte and ΔH_{PEO} is the heat of melting of 100% crystalline PEO, which is 213.7 J·g^{-1} [23, 24].

The composite solid-state electrolyte was punched into a circle with a diameter of 16 mm, and sandwiched between two stainless steel (SS) electrodes for the measurement of ionic conductivity, which was evaluated by an alternative current (AC) impedance spectrometer (Solartron 1260) in the range of 1 Hz–1 MHz over a temperature from 25 to 100 °C in 10 °C intervals on heating. Linear sweep voltammetry (LSV) test was conducted using an electrochemical workstation (CHI 660E) at a scan rate of 0.1 mV·s^{-1} to evaluate the electrochemical stability. The composite electrolyte was assembled in a lithium symmetric cell to evaluate Li^+ transference number (t_{Li^+}), which can be calculated by the following equation [28]:

$$t_{Li^+} = \frac{I_s(\Delta V - I_0 R_0)}{I_0(\Delta V - I_s R_s)} \quad (2)$$

where I_0 and I_s are the initial and steady state current, respectively, ΔV is the applied constant potential difference (20 mV), and R_0 and R_s are the interface impedance before and after polarization, respectively.

3 Results and discussion

3.1 Characterization of GF@HCS

The optical photos and SEM images of the dispersed GF and GF@HCS are shown in Fig. 2. From the optical photos, it is found that the color of the glass fiber changed from white to brown after the hydrothermal treatment, which is similar to the HCS reported previously [27, 29]. Moreover, from enlarged SEM images, it is observed that the surface of GF is very smooth, while the surface of GF@HCS is well-coated by a layer of ultrafine nanoparticles that are expected to be the HCS.

It is known that glucose will be dehydrated and polymerized into carbon nanospheres under the hydrothermal

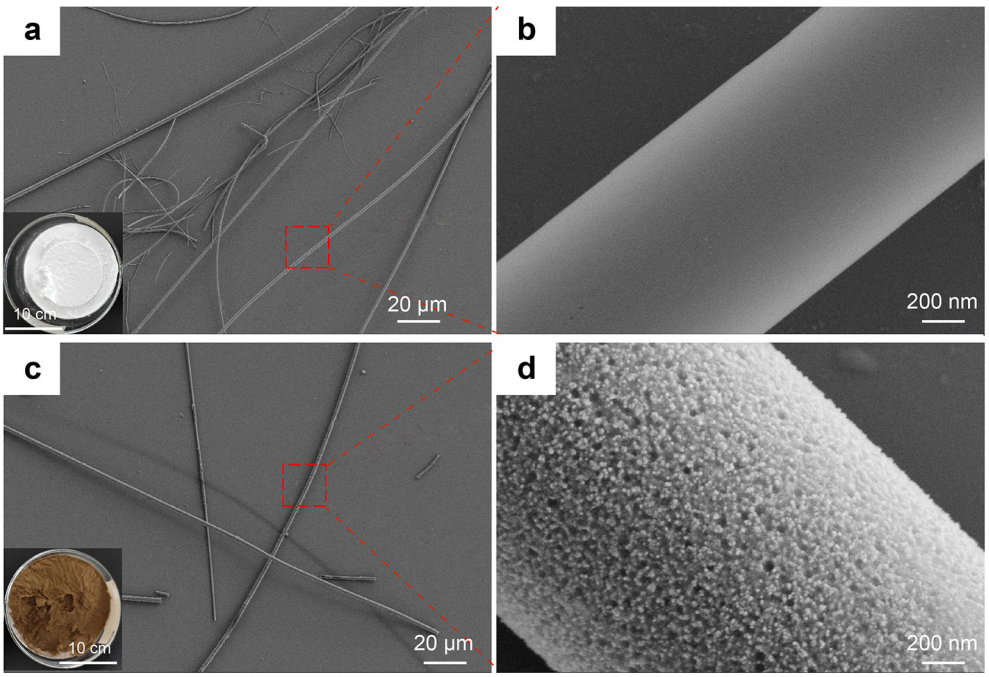

Fig. 2 SEM images of **a**, **b** GF and **c**, **d** GF@HCS fillers (insets showing corresponding optical photos)

condition. The surface of such HCS is enriched with oxygen-containing groups, such as hydroxyl, ester, ketone, as well as a small amount of alkene groups and phenyl groups. At present, it is generally believed that HCS is a core–shell configuration. The shell is mainly composed of oxygen-containing hydrophilic groups such as hydroxyl groups, and its carbon content is low; while the encapsulated core is mainly an amorphous carbon structure composed of oxygen-containing hydrophobic groups such as benzene ring, alkene and a small amount of ester groups [27]. To explore the nanoparticles coated on the surface of GF, FTIR curves of GF, GF@HCS as well as the pure HCS are compared (Fig. 3a). The broad infrared absorption peak at about 3430 cm^{-1} represents the stretching vibration of –OH. The two close peaks at 2920 and 2840 cm^{-1} are characteristics of the stretching vibration of CH_2 (aliphatic hydrocarbon), and those at 1750 and 1550 cm^{-1} signify the stretching vibration of C=O and C=C, respectively [30–32]. From FTIR spectra, the peaks corresponding to the vibration of CH_2 and C=O for pure HCS are clearly observed in GF@HCS, and the intensity of the –OH related peak in GF@HCS is much larger than that in GF, which can confirm successful modification of the glass fibers by HCS after the hydrothermal treatment. From the thermogravimetric curves in Fig. 3b, it can be seen that GF@HCS sample starts to decompose at about 300 °C, and the content of HCS grown on the GF is ∼ 2.2 wt%.

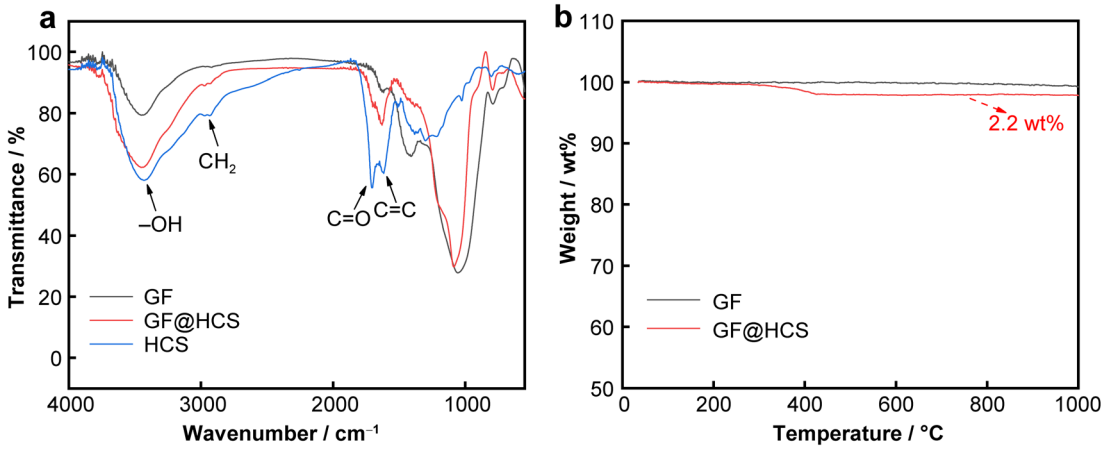

Fig. 3 **a** FTIR spectra of GF, GF@HCS and pure HCS; **b** thermogravimetric curves of GF and GF@HCS

3.2 Characterization of composite electrolyte

GF and GF@HCS fillers were, respectively, added into PEO16 to form a solid-state composite electrolyte. SEM images of the solid-state electrolyte with 2 wt% fillers (PEO16 + 2%GF and PEO16 + 2%GF@HCS) are shown in Fig. 4. Both GF and GF@HCS fillers are distributed in the entire PEO matrix and no essential morphological difference are observed for the two composite electrolytes.

The ionic conductivity of the composite electrolytes with different contents of fillers is shown in Fig. 5. It can be seen that over-addition of GF or GF@HCS fillers cannot continuously increase the conductivity of the electrolyte, which is similar to the reports on other nanoparticle fillers [1, 18]. The addition of 2 wt% is demonstrated as the best scenario, and the modification of GF seems to be beneficial for the ionic conductivity of the PEO-based electrolyte, especially at elevated temperatures. For example, at 60 °C, the conductivity of PEO16 + 2%GF@HCS is promoted to 4.4×10^{-4} S·cm^{-1}, being 400% higher than that of PEO16 (8.9×10^{-5} S·cm^{-1}), while for PEO16 + 2%GF, the conductivity at the same temperature is only 2.0×10^{-4} S·cm^{-1}. However, the room-temperature ionic conductivity of PEO16 + 2%GF and PEO16 + 2%GF@HCS is very close, being around 2.5×10^{-7} S·cm^{-1}. Eventually, the electrolyte with modified GF fillers (PEO16 + 2% GF@HCS) presents an ionic conductivity over twice that of the one with only GF (PEO16 + 2%GF) at 60 °C. These results reveal that the modification of GF with HCS can greatly enhance Li^+ transport in the PEO-based composite electrolyte at elevated temperatures. Such enhancement should originate from the increased amount of hydroxyl groups on HCS.

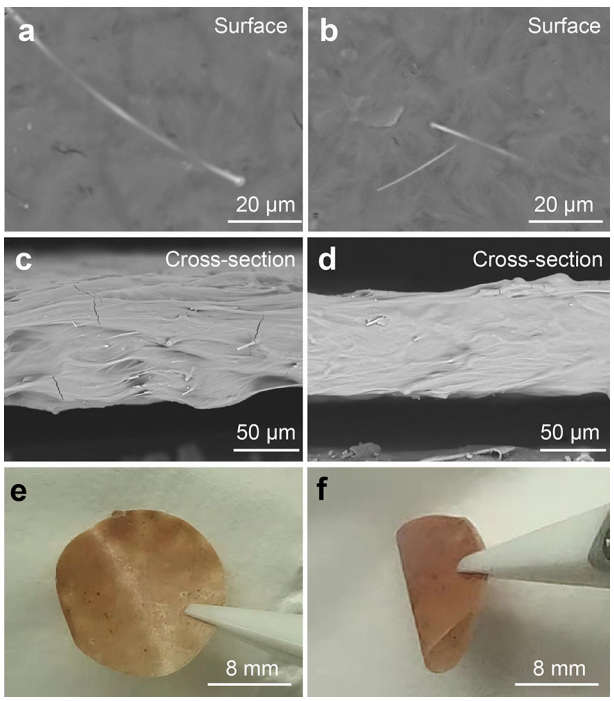

Fig. 4 Surface and cross-sectional SEM images of **a**, **c** PEO16 + 2%GF and **b**, **d** PEO16 + 2%GF@HCS composite electrolyte; **e**, **f** optical photos of PEO16 + 2%GF@HCS

In order to clarify the reason of the different ionic conductivity, differential scanning calorimetry (DSC) tests were conducted on different composite electrolytes and the results are shown in Fig. 6. By analysis of the DSC data, the physical properties of the composite polymers are calculated and listed in Table 1. We can see that after the addition of GF or GF@HCS fillers, T_m of all polymers is decreased, which is consistent with other literature reports [33]. However, X shows first an increase and then a decrease with the increase in the amount of GF and GF@HCS fillers, which may be caused by the aggregation of the micron-sized glass fibers, leading to an inhibition effect on the crystallinity of PEO [18]. As previously reported [1, 18], when a small amount of fillers are dispersed in the PEO matrix, the formation of spherulites in PEO can be effectively suppressed (meaning a decrease in crystallinity), while when the amount of fillers continues to increase, the fillers tend to aggregate and cannot be effectively dispersed in the PEO matrix, resulting in a weakening of the inhibitory effect of fillers, which is accompanied by an increase in crystallinity. The calculated X values of PEO16 + GF and PEO16 + GF@HCS are close to each other, which may be the reason that their room-temperature ionic conductivities are at the same level.

Steady-state current method was used to evaluate the t_{Li^+} of the PEO composite electrolyte at 60 °C. The electrochemical results are shown in Fig. 7a, b. The calculation reveals that t_{Li^+} values of PEO16 + 2%GF and PEO16 + 2%GF@HCS electrolyte are 0.12 and 0.18, respectively, indicating that the surface modification of GF by HCS can effectively promote the migration of Li^+. This conclusion is consistent with our previous work [26], and it is verified again that the oxygen atom in the hydroxyl group is helpful for the PEO matrix in terms of ion conduction. Figure 7c shows LSV curves of the PEO composite electrolytes with different fillers. It is observed that adding GF or GF@HCS fillers does not affect the electrochemical stability of the PEO16 polymer electrolyte. The decomposition voltage of both polymers is over 3.9 V, which enables their use in $LiFePO_4$-based solid-state batteries.

3.3 Cell performance

When lithium metal is used as the negative electrode, the energy density of the battery can be significantly increased.

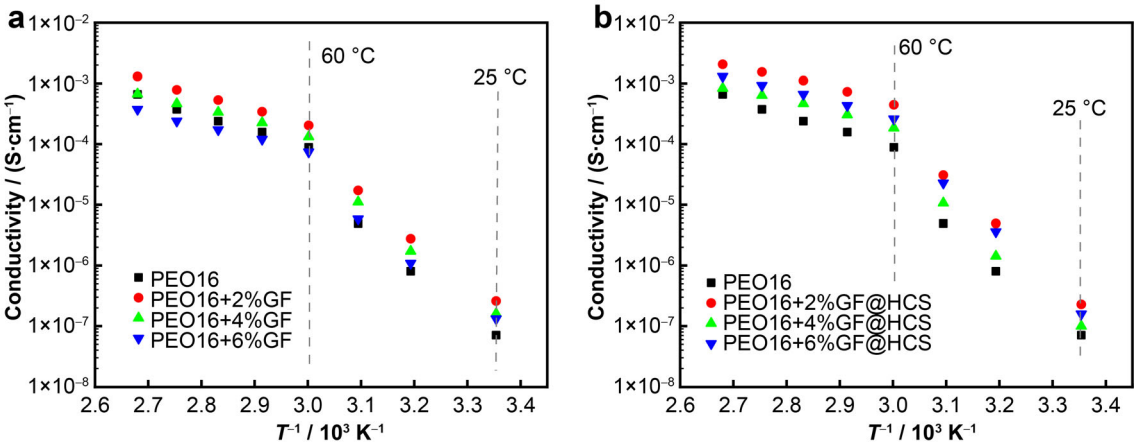

Fig. 5 Ionic conductivity of composite solid electrolytes with different amounts of **a** GF and **b** GF@HCS fillers

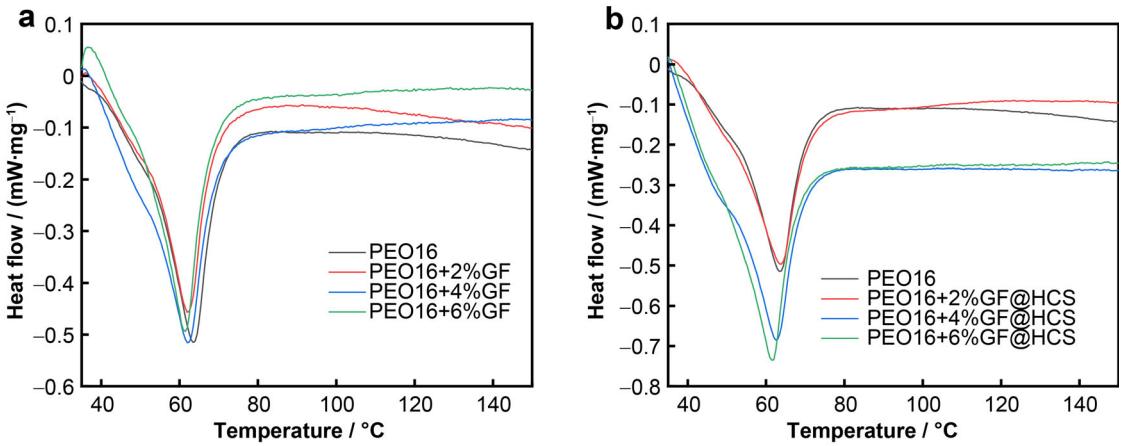

Fig. 6 **a**, **b** DSC curves of different composite electrolytes

Table 1 Physical parameters of PEO-based composite electrolytes calculated from DSC data

Sample	T_m / °C	$\Delta H_{m,PEO}$ / (J·g^{-1})	f_{peo} / %	X / %
PEO16	63.6	74.8	86.9	40.3
PEO16 + 2%GF	62.1	61.8	85.2	33.9
PEO16 + 4%GF	62.0	66.5	83.5	37.3
PEO16 + 6%GF	61.6	68.0	81.9	38.9
PEO16 + 2%GF@HCS	63.8	62.4	85.2	34.3
PEO16 + 4%GF@HCS	62.6	66.7	83.5	37.4
PEO16 + 6%GF@HCS	61.7	73.2	81.9	41.8

However, lithium metal has high reactivity and uneven deposition of lithium metal is easy to form lithium dendrites. The growth of lithium dendrites can cause short circuits and cause safety hazards. Therefore, it is also necessary to test whether the solid polymer electrolyte has good stability to lithium metal [34]. Figure 8 is potential-time curves of the Li/electrolyte/Li symmetric cells (0.1 mAh·cm^{-2}) deposited under different current densities. It is found that the PEO16 electrolyte with no fillers has a short circuit after 300-h cycling at 0.05 mA·cm^{-2}, while PEO16 + 2%GF and PEO16 + 2%GF@HCS electrolytes maintain good cycling stability. According to previous studies [24, 25], adding filler is able to improve the mechanical strength of the composite polymer electrolyte, which can be one reason of the improved cycling stability of these composite electrolytes. It is also seen that PEO + 2%GF@HCS has a relatively lower voltage polarization than PEO16 + 2%GF. For example, as the cycling lasts from 100 to 600 h, the polarization of PEO + 2%GF@HCS is kept as low as 0.074 V, while the polarization of PEO16 + 2%GF increases from 0.084 to 0.11 V. The less polarization of the symmetric cell is in consonance with the higher ionic conductivity of the PEO + 2%GF@HCS composite electrolyte at the elevated temperatures.

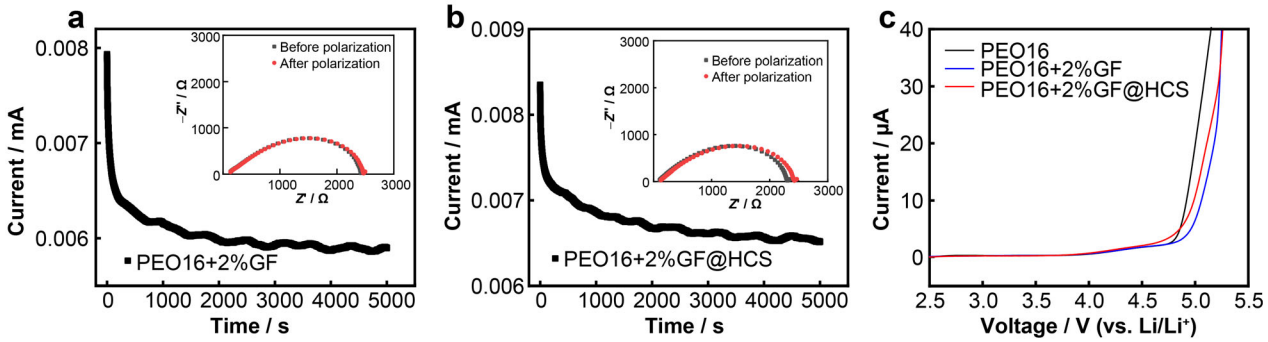

Fig. 7 Current relaxation curves of **a** PEO16 + 2%GF and **b** PEO16 + 2%GF@HCS composite electrolytes, and (insets) corresponding impedance diagrams before and after polarization; **c** LSV curves of composite electrolytes (all tests being performed at 60 °C)

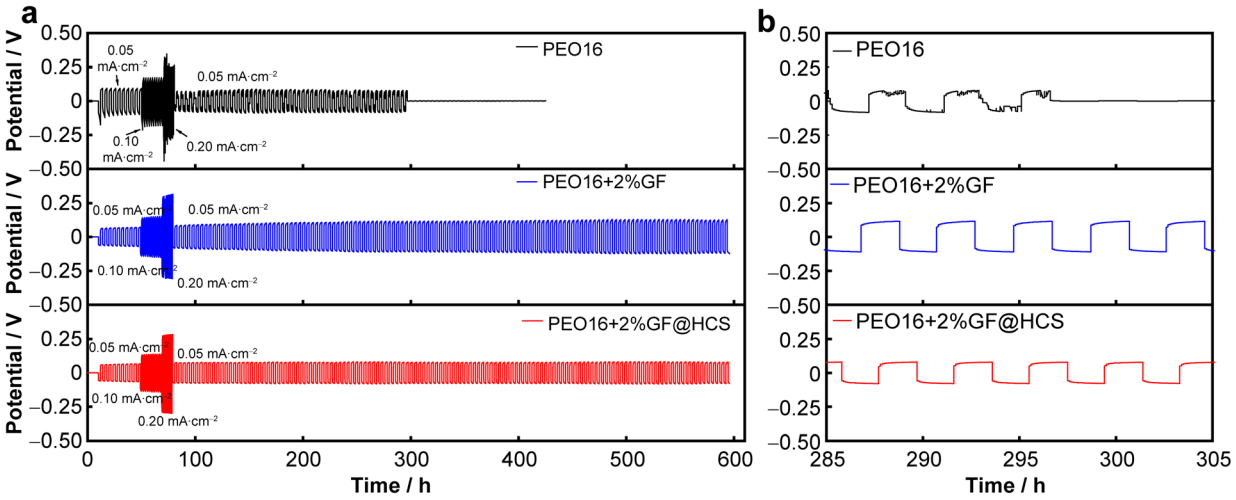

Fig. 8 **a**, **b** Potential-time profiles of Li/electrolyte/Li symmetric cells with deposition capacity of 0.1 mAh·cm^{-2} at 60 °C

The PEO composite polymers were also used as electrolyte in $LiFePO_4$/Li cells to evaluate their rate performances, which are shown in Fig. 9. The discharge capacity of the cells is significantly increased after the addition of both fillers. The addition GF@HCS is found to result in superior performance of the solid-state battery compared to the addition of only GF (Fig. 9a). The capacity of $LiFePO_4$/PEO16 + 2%GF@HCS/Li cell at 4.0C reaches 121 mAh·g^{-1}, which is obviously higher than those of the $LiFePO_4$/PEO16 + 2%GF/Li (112 mAh·g^{-1}) and $LiFePO_4$/PEO16 + 2%GF@HCS/Li (94 mAh·g^{-1}) cells. The enhancement of the high-rate performance is attributed to the higher ionic conductivity of the GF@HCS composite electrolyte, which leads to the lowest concentration polarization of the solid-state batteries (Fig. 9b, c).

The cycling performances of the batteries were also evaluated, as shown in Fig. 10. The solid-state batteries using all three composite electrolytes show a certain attenuation in capacity during cycling, which is probably due to unoptimized assembly of the solid-state battery. In the all-solid-state batteries, the traditional PVDF (as the binder) is absent because it cannot conduct Li^+. Instead, the ion-conductive PEO polymer is used as the binder in the electrode, but the adhesion of PEO polymer is poor, which may cause poor electrode/electrolyte contact and lead to fast degradation of the battery [35, 36]. Nevertheless, by comparing the cycling performances of the $LiFePO_4$/PEO16 + 2%GF @HCS/Li and $LiFePO_4$/PEO16 + 2%GF/Li cells, it can still be verified that the modification of GF by HCS is a beneficial strategy to improve the electrochemical performance of the PEO-based solid-state battery.

4 Conclusion

In this work, the positive effect of hydroxyl group on the conduction of Li^+ is evidenced in PEO-based solid-state electrolyte using HCS modified GF as a functional filler. With optimum addition of the GF@HCS filler (~ 2 wt%),

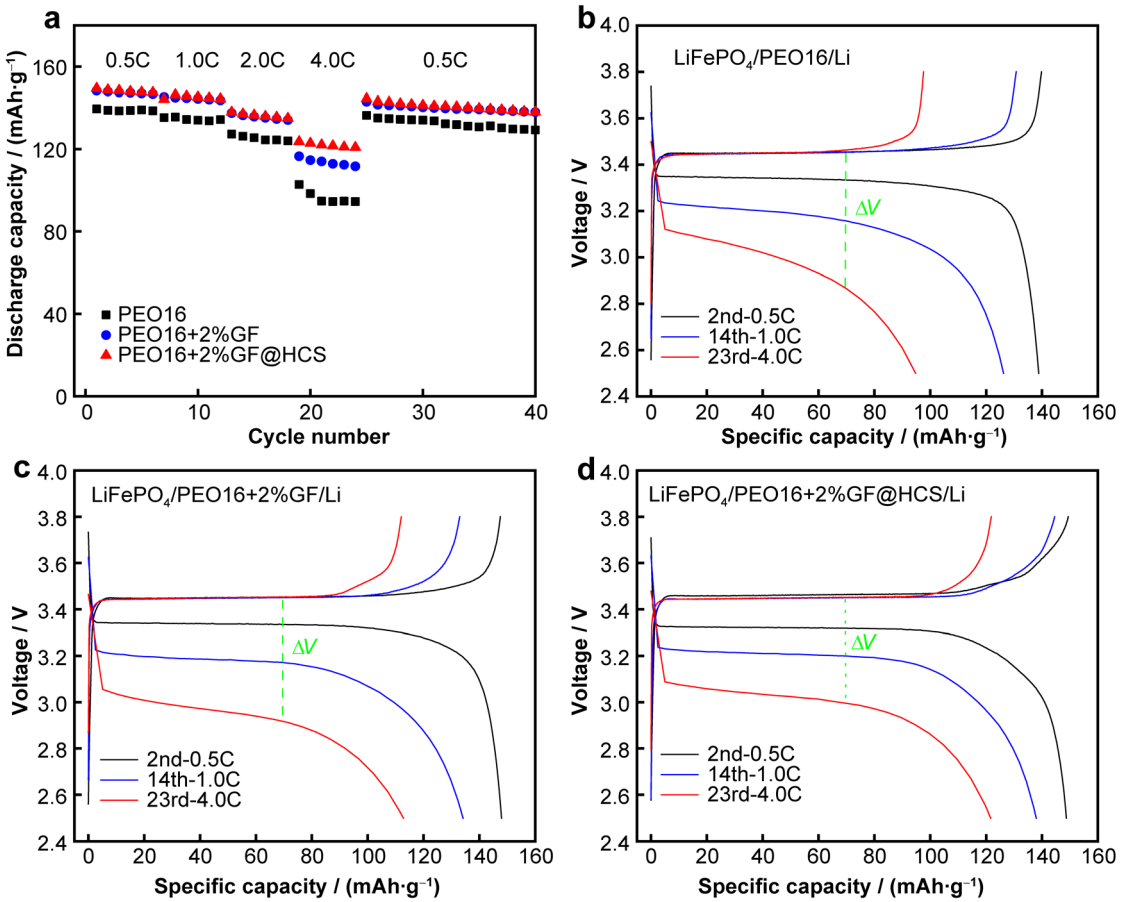

Fig. 9 **a** Rate performances of solid-state $LiFePO_4$/electrolyte/Li half-cells and **b**–**d** corresponding charge/discharge curves at different rates (all tests being performed at 60 °C)

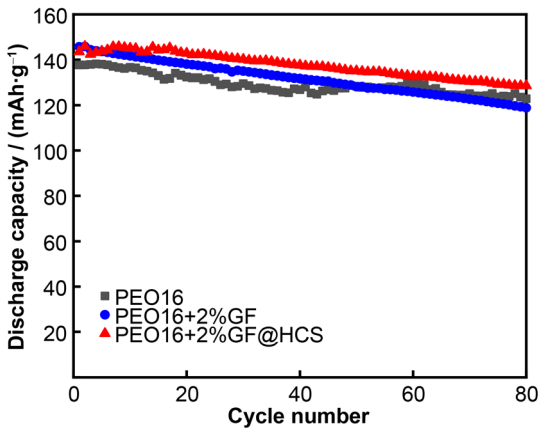

Fig. 10 Cycling performances of of $LiFePO_4$/electrolyte/Li all-solid-state batteries at 0.5C and at 60 °C

the ionic conductivity of the PEO composite electrolyte is increased from 8.9×10^{-5} to 4.4×10^{-4} S·cm^{-1} at 60 °C, being over twice that of the PEO electrolyte with only GF as the filler. Electrochemical tests reveal that the PEO16 + 2%GF@HCS composite electrolyte exhibits a high stability to lithium metal interface, and the $LiFePO_4$-based solid-state battery shows excellent rate performance at elevated temperature. This work opens a new way to modify one-dimensional nanowire fillers for the PEO-based solid-state electrolyte.

Acknowledgements This study was financially supported by the National Natural Science Foundation of China (Nos. 21875195, 22021001 and 52172184).

Declarations

Conflict of interests The authors declare that they have no conflict of interest.

References

[1] Zheng Y, Yao Y, Ou J, Li M, Luo D, Dou H, Li Z, Amine K, Yu A, Chen Z. A review of composite solid-state electrolytes for lithium batteries: fundamentals, key materials and advanced structures. Chem Soc Rev. 2020;49(23):8790. https://doi.org/10.1039/d0cs00305k.

[2] Cui J, Chen X, Zhou Z, Zuo M, Xiao Y, Zhao N, Shi C, Guo X. Effect of continuous pressures on electrochemical performance of Si anodes. Mater Today Energy. 2021;20:100632. https://doi.org/10.1016/j.mtener.2020.100632.

[3] Wei WQ, Liu BQ, Gan YQ, Ma HJ, Cui DW. Protecting lithium metal anode in all-solid-state batteries with a composite electrolyte. Rare Met. 2021;40(2):409. https://doi.org/10.1007/s12598-020-01501-6.
[4] Zhang XD, Yue FS, Liang JY, Shi JL, Li H, Guo YG. Structure design of cathode electrodes for solid-state batteries: challenges and progress. Small Struct. 2020;1(3):2000042. https://doi.org/10.1002/sstr.202000042.
[5] Zhou Q, Ma J, Dong SM, Li XF, Cui GL. Intermolecular chemistry in solid polymer electrolytes for high-energy-density lithium batteries. Adv Mater. 2019;31(50):1902029. https://doi.org/10.1002/adma.201902029.
[6] Ratner MA, Shriver DF. Ion-transport in solvent-free polymers. Chem Rev. 1988;88(1):109. https://doi.org/10.1021/cr00083a006.
[7] Wang Z, Shen L, Deng S, Cui P, Yao X. 10 μm-thick high--strength solid polymer electrolytes with excellent interface compatibility for flexible all-solid-state lithium-metal batteries. Adv Mater. 2021;33(25):2100353. https://doi.org/10.1002/adma.202100353.
[8] Guo Q, Xu F, Shen L, Wang Z, Wang J, He H, Yao X. Poly(-ethylene glycol) brush on $Li_{6.4}La_3Zr_{1.4}Ta_{0.6}O_{12}$ towards intimate interfacial compatibility in composite polymer electrolyte for flexible all-solid-state lithium metal batteries. J Power Sources. 2021;498:229934. https://doi.org/10.1016/j.jpowsour.2021.229934.
[9] Yang S, Zhang Z, Shen L, Chen P, Gu Z, Chang M, Zhao Y, He H, Yao X. Gravity-driven poly(ethylene glycol)@ $Li_{1.5}Al_{0.5}Ge_{1.5}(PO_4)_3$ asymmetric solid polymer electrolytes for all-solid-state lithium batteries. J Power Sources. 2022;518:23075. https://doi.org/10.1016/j.jpowsour.2021.230756.
[10] Papke BL, Ratner MA, Shriver DF. Vibrational spectroscopy and structure of polymer electrolytes, poly(ethylene oxide) complexes of alkali-metal salts. J Phys Chem Solids. 1981;42(6):493. https://doi.org/10.1016/0022-3697(81)90030-5.
[11] Adebahr J, Gavelin P, Jannasch P, Ostrovskii D, Wesslen B, Jacobsson P. Cation coordination in ion-conducting gels based on PEO-grafted polymers. Solid State Ionics. 2000;135(1–4):149. https://doi.org/10.1016/s0167-2738(00)00294-0.
[12] Mullerplathe F, Vangunsteren WF. Computer-simulation of a polymer electrolyte—lithium iodide in amorphous poly(ethylene oxide). J Chem Phys. 1995;103(11):4745. https://doi.org/10.1063/1.470611.
[13] Maitra A, Heuer A. Cation transport in polymer electrolytes: a microscopic approach. Phys Rev Lett. 2007;98(22):227802. https://doi.org/10.1103/PhysRevLett.98.227802.
[14] Dygas JR, Misztal-Faraj B, Floljanczyk Z, Krok F, Marzantowicz M, Zygadlo-Monikowska E. Effects of inhomogeneity on ionic conductivity and relaxations in PEO and PEO-salt complexes. Solid State Ion. 2003;157(1–4):249. https://doi.org/10.1016/s0167-2738(02)00217-5.
[15] Neat R, Glasse M, Linford R, Hooper A. Thermal history and polymer electrolyte structure—implications for solid-state battery design. Solid State Ion. 1986;18:1088. https://doi.org/10.1016/0167-2738(86)90314-0.
[16] Huang B, Li ZH, Zhu YM, Che Y, Wang CA. Tailored lithium metal/polymer electrolyte interface with $LiTa_2PO_8$ fillers in PEO-based composite electrolyte. Rare Met. 2022. https://doi.org/10.1007/s12598-021-01951-6.
[17] Jayathilaka P, Dissanayake M, Albinsson I, Mellander BE. Effect of nano-porous Al_2O_3 on thermal, dielectric and transport properties of the $(PEO)_9$LiTFSI polymer electrolyte system. Electrochim Acta. 2002;47(20):3257. https://doi.org/10.1016/s0013-4686(02)00243-8.
[18] Dissanayake M, Jayathilaka P, Bokalawala RSP, Albinsson I, Mellander BE. Effect of concentration and grain size of alumina filler on the ionic conductivity enhancement of the $(PEO)_9LiCF_3SO_3$:Al_2O_3 composite polymer electrolyte. J Power Sources. 2003;119:409. https://doi.org/10.1016/s0378-7753(03)00262-3.
[19] Croce F, Appetecchi GB, Persi L, Scrosati B. Nanocomposite polymer electrolytes for lithium batteries. Nature. 1998;394(6692):456. https://doi.org/10.1038/28818.
[20] Cheng Z, Liu T, Zhao B, Shen F, Jin H, Han X. Recent advances in organic-inorganic composite solid electrolytes for all-solid--state lithium batteries. Energy Storage Mater. 2021;34:388. https://doi.org/10.1016/j.ensm.2020.09.016.
[21] Chua S, Fang RP, Sun ZH, Wu MJ, Gu Z, Wang YZ, Hart JN, Sharma N, Li F, Wang DW. Hybrid solid polymer electrolytes with two-dimensional inorganic nanofillers. Chem A Eur J. 2018;24(69):18180. https://doi.org/10.1002/chem.201804781.
[22] Fan R, Liu C, He KQ, Cheng SHS, Chen DZ, Liao CZ, Li RKY, Tang JN, Lu ZG. Versatile strategy for realizing flexible room-temperature all-solid-state battery through a synergistic combination of salt affluent PEO and $Li_{6.75}La_3Zr_{1.75}Ta_{0.25}O_{12}$ nanofibers. ACS Appl Mater Interfaces. 2020;12(6):7222. https://doi.org/10.1021/acsami.9b20104.
[23] Liu W, Lee SW, Lin D, Shi F, Wang S, Sendek AD, Cui Y. Enhancing ionic conductivity in composite polymer electrolytes with well-aligned ceramic nanowires. Nat Energy. 2017;2(5):17035. https://doi.org/10.1038/nenergy.2017.35.
[24] Sheng OW, Jin CB, Luo JM, Yuan HD, Huang H, Gan YP, Zhang J, Xia Y, Liang C, Zhang WK, Tao XY. $Mg_2B_2O_5$ nanowire enabled multifunctional solid-state electrolytes with high ionic conductivity, excellent mechanical properties, and flame-retardant performance. Nano Lett. 2018;18(5):3104. https://doi.org/10.1021/acs.nanolett.8b00659.
[25] Lin Y, Wang XM, Liu J, Miller JD. Natural halloysite nano-clay electrolyte for advanced all-solid-state lithium-sulfur batteries. Nano Energy. 2017;31:478. https://doi.org/10.1016/j.nanoen.2016.11.045.
[26] Wang X, Hua H, Xie X, Zhang P, Zhao J. Hydroxyl on the filler surface promotes Li^+ conduction in PEO all-solid-state electrolyte. Solid State Ion. 2021;372:115768. https://doi.org/10.1016/j.ssi.2021.115768.
[27] Baccile N, Laurent G, Babonneau F, Fayon F, Titirici MM, Antonietti M. Structural characterization of hydrothermal carbon spheres by advanced solid-state MAS C-13 NMR investigations. J Phys Chem C. 2009;113(22):9644. https://doi.org/10.1021/jp901582x.
[28] Evans J, Vincent CA, Bruce PG. Electrochemical measurement of transference numbers in polymer electrolytes. Polymer. 1987;28(13):2324. https://doi.org/10.1016/0032-3861(87)90394-6.
[29] Sun XM, Li YD. Colloidal carbon spheres and their core/shell structures with noble-metal nanoparticles. Angew Chem Int Ed. 2004;43(5):597. https://doi.org/10.1002/anie.200352386.
[30] Chen Z, Ma LJ, Li SQ, Geng JX, Song Q, Liu J, Wang CL, Wang H, Li J, Qin Z, Li SJ. Simple approach to carboxyl-rich materials through low-temperature heat treatment of hydrothermal carbon in air. Appl Surf Sci. 2011;257(20):8686. https://doi.org/10.1016/j.apsusc.2011.05.048.
[31] Song XH, Gunawan P, Jiang RR, Leong SSJ, Wang KA, Xu R. Surface activated carbon nanospheres for fast adsorption of silver ions from aqueous solutions. J Hazard Mater. 2011;194:162. https://doi.org/10.1016/j.jhazmat.2011.07.076.
[32] Gong YT, Xie L, Li HR, Wang Y. Sustainable and scalable production of monodisperse and highly uniform colloidal carbonaceous spheres using sodium polyacrylate as the dispersant. Chem Commun. 2014;50(84):12633. https://doi.org/10.1039/c4cc04998e.
[33] Vignarooban K, Dissanayake MAKL, Albinsson I, Mellander BE. Effect of TiO_2 nano-filler and EC plasticizer on electrical and thermal properties of poly(ethylene oxide) (PEO) based

solid polymer electrolytes. Solid State Ion. 2014;266:25. https://doi.org/10.1016/j.ssi.2014.08.002.

[34] Lu Y, Zhao CZ, Yuan H, Cheng XB, Huang JQ, Zhang Q. Critical current density in solid-state lithium metal batteries: mechanism, influences, and strategies. Adv Funct Mater. 2021; 31(18):2009925. https://doi.org/10.1002/adfm.202009925.

[35] Nakayama M, Wada S, Kuroki S, Nogami M. Factors affecting cyclic durability of all-solid-state lithium polymer batteries using poly(ethylene oxide)-based solid polymer electrolytes. Energy Environ Sci. 2010;3(12):1995. https://doi.org/10.1039/c0ee00266f.

[36] Banerjee A, Wang X, Fang C, Wu EA, Meng YS. Interfaces and interphases in all-solid-state batteries with inorganic solid electrolytes. Chem Rev. 2020;120(14):6878. https://doi.org/10.1021/acs.chemrev.0c00101.